POLITECNICO MILANO 1863

SCUOLA DI INGEGNERIA INDUSTRIALE E DELL'INFORMAZIONE

PRELIMINARY DESIGN AND VERIFICATION OF A FUEL PIN

Nuclear Design and Technology project work

Department of Energy - Nuclear Engineering Division

Group 6: Pierluigi Faustini, Giorgio Galimberti, Giada Mazzoni, Gabriele Mentasti, William Oliveira, Elsa Charline Lucie Seichais, Patrik Shytaj.

---

1. Introduction

This technical report presents a comprehensive exploration of the preliminary design and verification process for a fuel pin within the scope of our project. The main general assumptions and design hypotheses are reported below:

- Focus on the worst possible condition: hot pin analysis
- Throttling that increases the mass flow rate by 1.3 times
- Negligible pressure losses and gravity in the coolant
- Thermal expansion evaluated using the average temperature

The main thermal analysis assumptions are:

- Thermal resistances approach
- No axial heat transfer
- Thin cladding approximation
- Only conductive heat transfer in the gap[1]
- The only consequence of restructuring is the accumulation of void in the center of the pellet

The main mechanical analysis assumptions are:

- Axial-symmetry and ortho-cylindricity
- Negligible volume forces
- Average values for α, ν, E
- Plane strain ϵ_z=0
- Safety limit S_a=$\frac{2}{3}\sigma_{yielding}$

The design choices are:

- The cladding thickness of size 0.5 mm
- The plenum height of size 50 cm.

2. Cold geometry

This first simulation treats the behaviour of the fuel in terms of a thermal analysis in cold geometry with a description and interpretation of each graph, along with the key takeaways from the outputs:

[1] Case of open gap

a) The graph shows the distribution of the linear heat rate along the fuel pin. The average linear heat rate is 34,910 W/m, which is a measure of the heat generated per unit length of the fuel pin.
b) The graph shows the corresponding axial temperature profile of the coolant, of the outer and inner cladding, and of the outer and inner fuel. The total temperature jump in the coolant is 185°C, suggesting the amount of heat absorbed by the coolant as it passes through the reactor core. The outlet temperature of the coolant of 585°C indicates the temperature while it exits the fuel assembly. The maximum outer cladding temperature which, to prevent cladding failure, must be below the design limit, is reported to be 590°C. Whereas, the maximum inner cladding temperature reaches 620°C; which is a significant figure since it represents the design limit for the cladding mid-wall temperature. The maximum outer fuel temperature is 1085°C and the inner fuel temperature reaches a peak of 2480°C, which is significantly higher than the outer temperature, suggesting a steep temperature gradient within the fuel. It provides a margin for melting of 553°C for the fuel, an indicator of the safety margin against fuel melting.
c) The graph shows the radial temperature gradients in the fuel, gap and cladding, referring to the worst case temperature axial position. This temperature profile is essential for assessing the thermal performance and ensuring that all parts of the fuel pin operate within safe temperature limits.

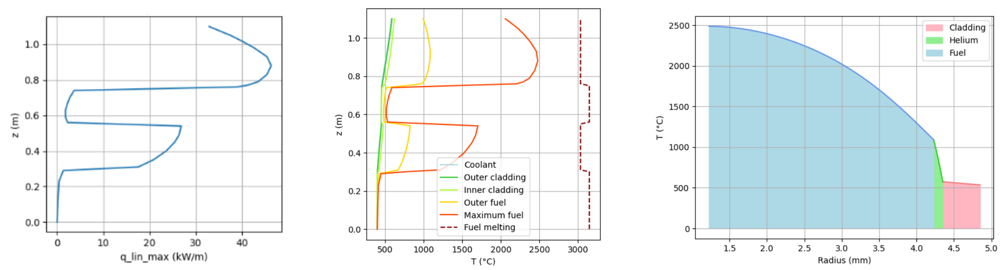

(a) Linear heat rate along the pin.

(b) Temperature distributions BoL.

(c) Radial temperature profile.

Figure 1: Thermal analysis cold geometry.

3. Hot geometry

The following paragraph highlights the differences and key points of the hot geometry analysis: the provided results are available for comparison with the cold geometry.

3.1. Thermal expansion effects

a) This graph shows how the radii expand due to thermal expansion of materials. The subsequent increase in surface area for heat transfer leads the temperatures across all components in the hot geometry to be generally lower than or similar to those in the cold geometry.
b) After accounting for thermal expansion, the temperatures in the cladding and fuel are slightly adjusted: the highest inner cladding temperature is still around 617°C, which is very similar to the cold geometry value of 620°C. The maximum outer fuel temperature after thermal expansion is 925°C, a marked decrease from the cold geometry value of 1085°C. The highest inner fuel temperature is 2335°C, which is also slightly lower than the cold geometry value of 2480°C.

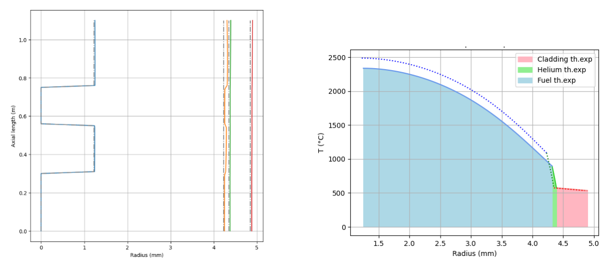

(a) Radii after thermal expansion.

(b) Radial temperature profile.

Figure 2: Thermal analysis after thermal expansion.

3.2. Restructuring effects

a) The calculated radii of the equiaxed grains region, columnar grains region, and void region, are critical for understanding the microstructural behavior of the fuel under thermal conditions.
b) The graph produced shows the temperature distribution across the radial distribution of the different grain structures within the fuel. These visual representations enable the identification of any potential issues related to heat transfer and material integrity.
c) After accounting for both thermal expansion and material restructuring, another thermal expansion has been simulated since the thermal process is iterative. The maximum outer cladding temperature remains virtually unchanged from the first part of the hot geometry analysis at 590°C. The highest inner cladding temperature has slightly decreased to 618°C from 620°C in the cold geometry. Regarding the maximum outer fuel temperature, it shows a small increase from the first part of the hot geometry analysis to 930°C but is still lower than the 1085°C observed in the cold geometry. Concerning the highest fuel inner temperature,it highlights a considerable decrease to 2250°C from 2480°C in the cold geometry. The as-fabricated region's maximum temperature is 1525°C. The equiaxial region's maximum temperature is 1715°C. The columnar region's peak temperature is 2220°C. With respect to the temperatures across the cladding in the hot geometry, a decrease compared to the cold geometry can be observed. This indicates that the cladding material handles the thermal expansion well without significant changes in temperature profiles. The decrease in the inner fuel temperature in the hot geometry analysis is notable. It suggests that the restructuring and expansion of the fuel material under high temperatures can potentially lead to a reduction in the temperature within the fuel, thereby enhancing the safety margin. The detailed temperatures in the as-fabricated, equiaxial, and columnar regions indicate that the fuel's internal structure has a significant impact on its thermal behavior. Regarding the columnar region, it shows the highest temperature, which could be a point of interest for material integrity under real reactor conditions.
d) Overall, the hot geometry analysis, with its focus on thermal expansion and restructuring, gives a more dynamic and realistic picture of the fuel pin's behavior under operational temperatures.

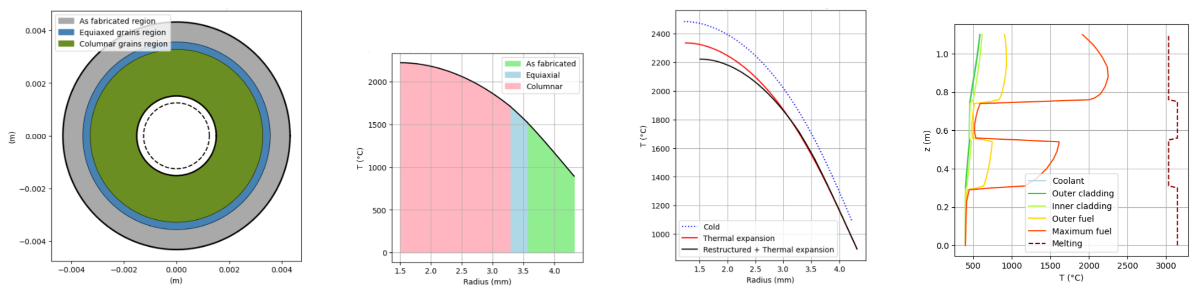

(a) 3 zones of restructuring.

(b) Radial temperature profile.

(c) Cold - Thermal expansion - Restructuring: Radial profile

(d) Axial temperature profiles.

Figure 3: Thermal analysis after restructuring.

4. Mechanical analysis at the beginning of life

The mechanical analysis provides insights into the stress behaviors under different conditions in the cladding of the nuclear fuel pin. The graphs depict how radial, circumferential and axial stresses vary along the radius of the cladding. Here are the highlights focusing on the stress output, which has been compared with the safety limit across all points. This implies that the maximum shear stress (Tresca stress) at any point in the cladding must not exceed the material's yield stress:

a) In the scenario where only thermal stresses are considered, the results suggest that the stress within the cladding remains under the safety limit across all the axial points. Hence the material can withstand the thermal stresses induced by temperature gradients without reaching the yield stress or failing.
b) When considering only mechanical stresses, which are due to internal and external pressures (0.35 MPa inner and 0.3 MPa outer), the stress again stays under the safety limit in all the axial points of the cladding. This suggests that the cladding can withstand the mechanical loading without yielding or failing.
c) For the combined effect of mechanical and thermal stresses, the output indicates that the stress remains under the safety limit for all the axial points along the cladding. This is a crucial aspect of the design, as it demonstrates the cladding's ability to withstand the realistic operational conditions where both thermal

and mechanical stresses are present.
Thus, according to the Tresca criterion, the cladding is deemed safe from yielding under the given thermal and mechanical load conditions.[2]

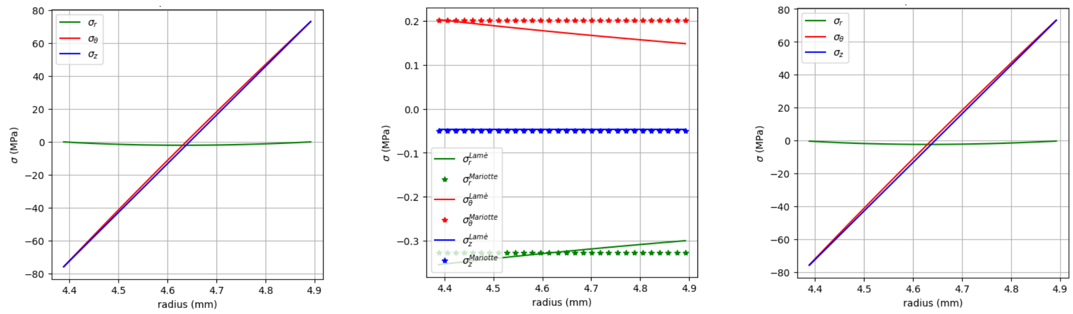

(a) Radial profiles of thermal stresses.

(b) Radial profile of mechanical stresses.

(c) Radial profile of total stresses.

Figure 4: Thermal - Mechanical - Total stresses BoL.

5. Plenum design

The analysis of fission gas production and plenum sizing has provided us with various results related to the behavior of fission gases within the nuclear reactor fuel rod. We have assumed that only Xenon and Kripton are produced in the fuel pin as fission gasses. The following insights based on the outputs have been observed:

a) A total of $2.2 \cdot 10^{22}$ atoms of fission gas have been produced. This figure represents the cumulative number of fission gas atoms generated and it is a key factor in understanding the volume of gas that must be managed within the fuel rod. The percentages of Xenon (Xe) and Krypton (Kr) released from the fuel are provided. In the two fertile fuel pellets we have evaluated that there is no release of fission gas. On the other hand the upper fissile fuel pellet shows a release of 100 % since its temperature is very high and the fission gases diffuse towards the boundaries. This contributes to the escape from the fuel matrix into the gap or plenum. Lastly the first fissile fuel pin which is at lower temperature shows a quite low release.

b) To design the plenum, however, the worst case scenario has been considered, and so a 100% release of fission gas has been assumed. There are about $8.3 \cdot 10^{20}$ atoms of Helium (He) in the gap, which translates to a mass of approximately 0.0055 grams. The mass of Xenon in the gap is about 4.37 grams, and Krypton is about 0.31 grams. These masses are important for calculating the pressure in the gap and ensuring that the cladding can withstand this pressure without failure. The tentative value for the height of the plenum has been assumed of 50 cm. A pressure value inside the plenum of approximately 3.80 MPa has been calculated . This pressure is within the design limits indicated earlier ($<$ 5 MPa), suggesting that the plenum has been sized correctly to accommodate the fission gas release without exceeding safety limits. The value of temperature used to design the plenum has been assumed to be of 400°C, referring to the inlet temperature of the coolant. This is because the coolant temperature is not affected by the fission gases since their release is distributed through 4 years; the daily emission is marginal. Thus, the plenum is supposed to be a lower plenum. Some fission gas, then, will accumulate also in the upper plenum, which is usually present to accommodate the spring. The axial expansion is calculated to be approximately 16 mm. This mechanical change in the fuel rod is crucial for the physical integrity of the fuel assembly and must be accounted for in the design to avoid undue stresses. This must be taken into account when designing the upper plenum.

[2]These plots are related to the most stressed axial position

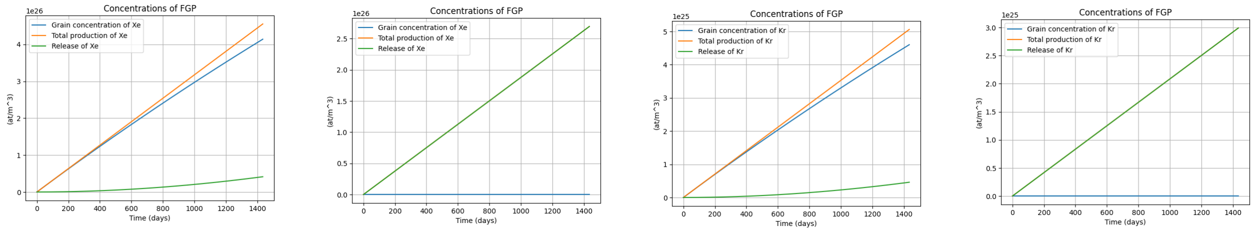

(a) First Fissile Xe Release. (b) Second Fissile Xe Release. (c) First Fissile Kr Release. (d) Second Fissile Kr Release.

Figure 5: Fission Gas Release.

6. Burnup analysis

A comprehensive time-dependent analysis enables us to predict heat, radiation, and mechanical stress changes over time, ensuring the fuel pins perform safely and efficiently throughout their lifecycle.

6.1. Contact pressure

a) The graph is a detailed representation of the contact pressure evolution in a nuclear reactor fuel pin. It provides a nuanced view of how the fuel, undergoing thermal expansion and radiation-induced swelling, begins to exert increasing pressure on the cladding.
b) This pressure is not constant but varies along the length of the pin. Key points in the graph indicate where the pressure peaks, which are critical for understanding the mechanical stresses exerted on the cladding.

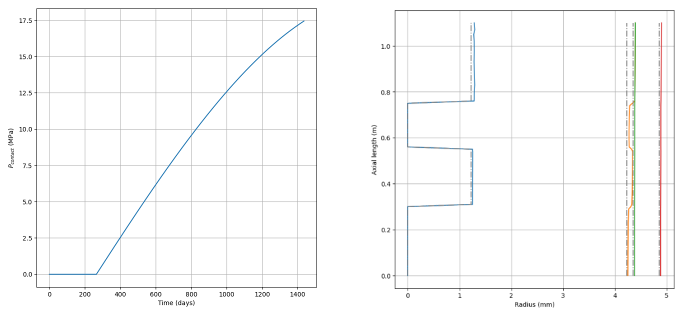

(a) Contact pressure. (b) Radius after irradiation.

Figure 6: Contact pressure and new radii.

Safety margins for cladding volumetric swelling indicate that the limits are respected, as the values are below 6%. In a more realistic picture of the fuel-cladding contact pressure's behaviour under operational temperatures and irradiation history, the gap should re-opens due to the fuel contraction caused by the cooling of the fuel after having contact with the cladding. However, we have neglected for simplicity this behavior, imposing that the contact remains.

6.2. New temperature profile after 4 years

This graph maps the temperature profile across the fuel pin at the end of the reactor's life. The overall temperature range at the end of life is higher than during normal operation, suggesting material degradation and increased fission product buildup. It is possible to notice a totally different profile of the outer fuel temperature in the axial positions corresponding to the upper fissile pellet: this is due to the pellet-cladding contact. In this region the gap disappears and the heat transfer is due to the contact: the value used for the heat transfer coefficient is $1\frac{W}{m^2K}$ [2]. In a more realistic picture we expect the fuel pin temperature to decrease along the life of the reactor, as the linear power decreases in time. However, we have neglected for simplicity the restructuring effects along time, which would have decreased the temperatures. Thus, due to the fission gas release which leads to the degradation of the gap conductivity the temperatures increase. Moreover, the burnup rising results in the worsening of the thermal conductivity of the fuel and therefore the temperatures increase.

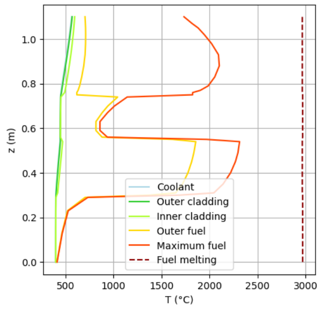

Figure 7: Temperature distributions EoL

7. Mechanical analysis at the end of life

At the reactor's end of life, the fuel pins have been subjected to prolonged exposure to radiation, heat, and mechanical stresses. This prolonged exposure leads to increased material degradation, higher thermal stresses due to changes in fuel and cladding properties and alterations in mechanical stresses due to changes in the reactor's internal environment. Having verified with Tresca criterion the yield stress, we can conclude that the fuel pin can withstand not only the initial operating conditions but also the more challenging conditions of the end of its life.[3]

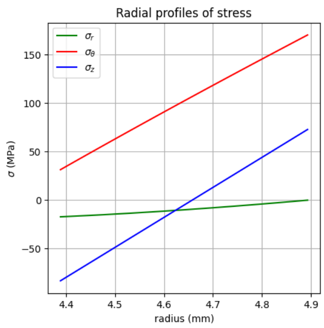

Figure 8: Radial profile of total stresses EoL

8. Thermal creep strain verification

Thermal creep is a time-dependent phenomena: to verify that its value for the cladding is below the safety limit, we need to consider a cumulative thermal creep strain during the operational life. Each time interval has a given strain value characterized by a specific stress and temperature state. The verification for the equivalent stress leading to creep failure has been performed using the Larson-Miller parameter, which has required the calculation of the Von Mises equivalent stress. The results show that both at the beginning and at the end of life, the temperature, the time and the stresses are below the safety limits.
The cladding thermal creep strain always satisfies the safety limit of 0.2% and the worst axial points safety margins are at the beginning of life 0.19907% and at the end of life 0.19411%.

9. Helium embrittlement

The Helium concentration in parts per million (ppm) after 1 year is provided along the axial length of the fuel rod. The concentration varies significantly, with higher concentrations towards the middle of the fuel rod, which can affect material properties such as thermal conductivity and specific heat capacity. The Helium concentration axially spans from a minimum of 0.044 ppm to a maximum of almost 44 ppm.

[3] This plot is related to the most stressed axial position

References

[1] Maurizio Luigi Cumo. *Nuclear plants.* Università Sapienza Editrice, 2017.

[2] Olander Donald. *Fundamental Aspects of Nuclear Reactor Fuel Elements.* Technical Information Center, Office of Public Affairs Energy Research and Development Administration, 1976.

[3] Hamilton Duderstadt. *Nuclear Reactor Analysis.* 1976.

[4] Elsevier. *Elements of Nuclear Reactor Design.* 1977.

[5] Sesonke Glasstone. *Reactor Design Basics.* 1994.

[6] Lelio Luzzi. Comportamento dei materiali sotto irraggiamento neutronico nel nocciolo di un reattore nucleare.

[7] Lelio Luzzi. Thermomechanics.

[8] Linga Murty and Indrajit Charit. *An Introduction to Nuclear Materials.* 2012.

[9] Todreas-Kazimi. *Nuclear System I, Thermal Hydraulic Fundamentals.* 1993.